Environmental Research 215 (2022) 114393

Contents lists available at ScienceDirect

Environmental Research

journal homepage: www.elsevier.com/locate/envres

Natural and human factors influencing urban particulate matter concentrations in central heating areas with long-term wearable monitoring devices

Chuyi Zhang [a,b,c], Yuanman Hu [a], Matthew D. Adams [c], Miao Liu [a], Binglun Li [a], Tuo Shi [d], Chunlin Li [a,*]

[a] CAS Key Laboratory of Forest Ecology and Management, Institute of Applied Ecology, Chinese Academy of Sciences, No. 72, Wenhua Road, Shenyang, 110016, China
[b] College of Resources and Environment, University of Chinese Academy of Sciences, No. 19, Yuquan Road, Beijing, 100049, China
[c] Department of Geography & Planning, University of Toronto, 3359 Mississauga Road, Mississauga, ON, L5L 1C6, Canada
[d] College of Life Science, Shenyang Normal University, No. 253 Huanghe North Street, Shenyang, 110034, China

ARTICLE INFO

Keywords:
Wearable sampling
Heating/non-heating season
Fine urban particulate matter
Human activity
Random forest model

ABSTRACT

In northern China, central heating, as an important source of urban particulate matter (UPM), causes more than half of the air pollution during the heating season and has significant spatial-temporal heterogeneity. Owing to the limitations of stationary air monitoring networks, few studies distinguish between heating/non-heating seasons and few have been conducted in urban areas. However, fixed monitoring cannot accurately capture the dynamic exposure of residents to UPM, and there is a lack of comprehensive evaluation of the factors affecting UPM. Therefore, this study used wearable Sniffer 4D equipment to monitor the concentrations of UPM (PM_1, $PM_{2.5}$, and PM_{10}) in selected typical areas of Shenyang City from March 2019 to February 2020. A random forest model was combined with land use and point-of-interest data to analyze the contributions and marginal effects of multiple influences on UPM, in both heating and non-heating seasons. The results showed that in the eastern part of the study area, UPM showed completely opposite spatial distribution characteristics during the two seasons. The concentrations of UPM were higher during the heating season than during the non-heating season. The results indicated that temperature and humidity were important factors in diffusing UPM. The production and operation of boilers were important for the production of UPM. In two-dimensional landscape pattern indices, the percentage of forest and Shannon diversity index were the first and second most important factors, respectively. The three-dimensional pattern of buildings had important effects on the transport and diffusion of UPM (landscape height range >100, floor area ratio >1.3, and landscape volume density >5). Wearable devices could monitor the real situation of residents' exposure to UPM and quantify the factors influencing the spatial-temporal distribution of UPM in an ecological sense. These results provide a scientific basis for urban planning and for health risk reduction for residents.

1. Introduction

China has undergone rapid urbanization, with the urbanization rate of permanent residents increasing from 10.64% in 1949 to 63.89% in 2020 (China, 2020). The extensive and inefficient pattern of economic development has severely damaged the ecological environment. Despite an increase from 83.1% in 2016 to 87.0% in the average proportion of "good" urban air quality days (AQI <100) across China in 2020 (Zhang et al., 2021), extreme air pollution events, such as heavy haze, still occur in specific seasons and regions (Chen et al., 2021; Li et al., 2019; Wang et al., 2019). Haze occurs when particulate matter less than 2.5 μm in aerodynamic diameter ($PM_{2.5}$) accumulates in the atmosphere, reducing visibility (An et al., 2019; Gao et al., 2017a). Because of its small size, $PM_{2.5}$ penetrates deep into various bodily systems, chronic low-concentration inhalation and acute high-concentration inhalation can adversely affect people's health, causing neurological and fetal damage as well as respiratory and cardiovascular disease (Althuwaynee et al., 2020; Azarmi et al., 2016; Weichenthal et al., 2020). This increases the risk of chronic diseases and cancer, premature death, and respiratory damage (Khomenko et al., 2021; Kim et al., 2015; Pope et al.,

* Corresponding author.
E-mail address: lichunlin@iae.ac.cn (C. Li).

https://doi.org/10.1016/j.envres.2022.114393
Received 25 June 2022; Received in revised form 16 September 2022; Accepted 18 September 2022
Available online 21 September 2022

2020), as well as health care needs and reduces quality of life (Chen and Chen, 2021). In addition, the environmental effects of urban particulate matter (UPM) include reduced environmental benefits and a range of ecological problems caused by blocking sunlight; it may also act as an impediment to economic development (Gao et al., 2017a; Khomenko et al., 2021; Pope et al., 2020). Therefore, there is an urgent need to control UPM, for both human health and ecological environment protection reasons.

The primary anthropogenic sources of UPM within cities include industrial, traffic, and residential emissions (Karagulian et al., 2015; Liu et al., 2016). Petroleum and coal are typical winter energy sources for central heating in most of China north of 34°N (Shi et al., 2018). More than half of the air pollution in northern China originates from residential heating (Lin and Ling, 2021). This unique anthropogenic influence in the middle and high latitudes creates additional seasonal characteristics in the heating (HS) and non-heating (NHS) seasons, which differ from the regular four seasons of the year (Wang et al., 2019). As a result, the spatial-temporal distribution patterns of UPM are higher in the HS than in the NHS, and higher in the north than in the south (Liu et al., 2019; Pang et al., 2021; Wang et al., 2018; Zhao et al., 2016). This causes higher health risks for urban residents in the HS than in the NHS (Qu et al., 2019). Previous studies of HS and NHS were conducted at the national and city group levels but were unable to characterize the complex air pollution changes within cities (Chen et al., 2021; Wang et al., 2018; Yang et al., 2016). Therefore, studying the spatial-temporal distribution of UPM at entire city or urban precinct scales is of great importance for urban planning and residential health (Shi et al., 2020), including distinguishing the characteristics of air pollution during different seasons and conducting related studies within urban areas.

The monitoring of air pollutants can be divided into fixed-station monitoring and mobile equipment monitoring. Data from fixed urban monitoring stations have the advantage of high time continuity and are thus widely used (Xie et al., 2017). However, owing to construction and maintenance costs and other reasons, monitoring stations are unevenly distributed within cities (Castell et al., 2017). Therefore, they cannot meet the needs of fine-scale pollutant concentration studies in cities (Kumar et al., 2015; Rai et al., 2017). Mobile monitoring equipment has emerged to fill this gap and provide data that accurately represent the exposure of the population (Bulot et al., 2019; Jovasevic-Stojanovic et al., 2015; Karagulian et al., 2019). This mobile equipment simplifies monitoring operations and allows users to complete monitoring activities without the need to learn complicated technical skills (Karagulian et al., 2019). These mobile sensors provide local information for decision makers and urban residents (Mahajan and Kumar, 2020). The primary mobile monitoring method is vehicle monitoring; however, there are spatial differences in pollutant concentrations between motorways and sidewalks, and it cannot accurately assess the concentrations of pollutants to which residents are exposed (Cao and Thompson, 2017; Pattinson et al., 2017; Rakowska et al., 2014). Wearable devices worn by volunteers are small and inexpensive and can monitor air pollution on sidewalks (Helbig et al., 2021; Mallires et al., 2019), which can then feed into a database for studies requiring data with high spatial-temporal resolution (Morawska et al., 2018; Rivera et al., 2012). However, most of the studies conducted using this approach have been in Europe, with similar research in Asia lacking, especially in highly polluted and densely populated areas (McKercher et al., 2017). Meanwhile, short-term small-area, high-precision monitoring and long-term large--area, low-precision monitoring are still common data sources used in studies (Helbig et al., 2021; Mallires et al., 2019). Because of feasibility, long-term series data monitoring and wearable mobile monitoring were not chosen simultaneously. The acquisition of long-term, high-precision UPM data remains a challenge for researchers studying urban air pollution.

Factors influencing UPM with high spatial-temporal heterogeneity are complex and diverse. Natural factors significantly impact air pollution, particularly meteorology (Li et al., 2020). City UPM is sourced from traffic (25%), household fuel combustion (20%), and industrial activity (15%) (Karagulian et al., 2015). Landscape patterns describe the type and diversity of landscape component units and their spatial relationships (Chen et al., 2006). The influence of 2D and 3D landscape pattern indices on $PM_{2.5}$ concentration distribution is significant (explanatory power up to 33.85% and 40.94%, respectively; Ke et al., 2022), and are mainly related to the distribution of parks and water bodies, building and population density, traffic, and land cover (Weng and Yang, 2006). Green land significantly limits the spread of particulate matter within 100–500 m buffers, and more compact and continuous green land contributes to the reduction of air pollution (Greenstone et al., 2022; Lowicki, 2019). Dense high-rise buildings provide a barrier to the transport and diffusion of air pollution (Weber et al., 2014). The concentration of UPM in deep, narrow street valleys is significantly lower than that in wide street valleys (Miao et al., 2020; Shi et al., 2020). Although previous studies have analyzed various aspects of the factors influencing UPM, comprehensive and integrated studies on the influencing factors affecting the spatial-temporal distribution of UPM are still lacking. Moreover, quantitatively revealing the correspondence between patterns and processes has been a challenge in landscape ecology (Wu and Hobbs, 2002). Although previous studies have provided qualitative analyses of landscape patterns and pollutant distribution processes, quantitative analysis can provide better support for improving landscape patterns so the urban environment can better mitigate the effects of UPM pollution (Wu, 2013).

Therefore, combining multiple factors could enhance the investigation of the impact mechanisms of urban air pollution. Among multivariate relationship analyses, random forest (RF) is considered a classification tree-based algorithm with high accuracy (Breiman, 2001; Hu et al., 2017; Ma et al., 2020b). Although the RF method has unexplained similarities to the black-box model, it is still widely used in many air pollution modeling studies due to its fast training speed and easy parallelization (Vu et al., 2019). Although the simulation prediction of pollutant concentrations is currently the main use of RF models, another advantage of RF is that it can calculate the importance estimates for each predictor variable; additionally, the RF model does not need to check for covariance or normalize data for different magnitudes (Rahman and Islam, 2019; Strobl et al., 2008).

In this study, wearable air pollution monitors were used to conduct long-time series of high-resolution UPM monitoring activities on sidewalks in the built-up area of Shenyang City. This study considered the factors influencing pollutant generation, transmission, and dispersion. The objective was to quantitatively reveal the relationships between natural factors, human activities, and two-dimensional (2D) and three-dimensional (3D) landscape patterns on UPM using the RF method. To distinguish the changes in the concentrations of UPM between HS and NHS, seasonal variations were considered in this study.

2. Materials and methods

2.1. Study location and experimental design

The study was conducted in Shenyang City, northeast China, in the middle of Liaoning Province. It has a temperate, semi-humid continental climate, with a large annual temperature difference and four distinct seasons. Shenyang, located in the center of the Liaohe Plain, provides meteorological transport and diffusion because the terrain is flat, the average altitude is approximately 50 m, and the maximum elevation difference in the city is 29 m. The number of days with winds greater than 6 m/s (wind speed is 10.8–13.8 m/s) is concentrated in spring, accounting for approximately 46% of the annual number of windy days (http://www.weather.com.cn/cityintro/101070101.shtml). However, owing to its dense internal population and large-scale industrial enterprises, Shenyang has high emissions of various atmospheric pollutants (Guo et al., 2021; Ma, 2021). Shenyang, the capital of Liaoning

Province, has the second-highest particulate emissions in China, with industrial and domestic sources as the primary pollution sources. Heavy industry and coal-fired heating in winter lead to frequent extreme air pollution, with 105 air pollution days in Shenyang in 2020 (Administration, 2021; Chang et al., 2020). Thus, to explore the influence of human activities on the concentration of air pollutants, typical areas were selected in the center of Shenyang City, including parks, commercial areas, residential areas, tourist attractions, hospitals, and schools. Overall, the selected study area has diverse land use types representing a range of urban characteristics of the city.

The air pollution monitoring data used in this study were obtained using Sniffer4D wearable atmospheric mobile monitoring equipment produced by Soarability Technologies. The UPM acquisition module (Plantower, model PMplantower 003) operates with a miniature laser photometer based on the laser scattering principle (Li et al., 2020). With a resolution of 1 μg/m^3 and range of 0–1000 μg/m^3, the humidity correction algorithm was embedded in the module chip. Sniffer4D atmospheric mobile monitoring equipment has the characteristics of small size, ease of use, anti-electromagnetic interference, excellent internal structure damping, high sensitivity, and it passes the authority test of the national measurement center. The sampling frequency is once per second, and the average error of the sampling data is $<\pm$ 10% compared with scientific-level air monitoring stations; the long-term data correlation (R^2) is 0.81–0.95 (www.soarability.tech/sniffer4dV2_hardware). The monitoring of UPM was performed by three volunteers using the same wearable monitoring equipment in succession every day from March 2019 to February 2020. For stable sampling, the monitor was worn 1.5 m above the ground (Fig. 1) with a sampling interval of 1 s (Choi et al., 2018). Five parameters were obtained: temperature (°C), relative humidity (%), PM_1 (μg/m^3), $PM_{2.5}$ (μg/m^3), and PM_{10} (μg/m^3). Before daily sampling, the equipment was placed in the same environment as the national standard monitoring station and then calibrated (Li et al., 2020). Due to the use conditions of the equipment and because of research needs, rainy days were not monitored. Owing to the portability of handheld devices, volunteers used the sidewalk (Fig. 1); therefore, the sampling period was not affected by morning and evening peak traffic. The entire sampling process was conducted from 7 a.m. to 7 p.m. and strictly compliant with the Road Traffic Safety Law of the People's Republic of China (http://www.gov.cn/zhengce/2020-12/27/content_5574617.htm).

2.2. Selection of influencing factors

In this study, 37 impact factors were used to analyze the effects of comprehensive factors on UPM concentrations from several aspects (Table 1). As mentioned before, temperature and humidity significantly impact air pollution (Li et al., 2020), human activity affects UPM generation and transmission (Karagulian et al., 2015), and 2D and 3D landscape pattern indices can significantly affect UPM concentration distribution (Ke et al., 2022). For human activity, point of interest (POI) data can represent different spatial-temporal patterns (Gao et al., 2017b). For 2D and 3D landscape pattern indices, those related to air pollution were selected (Ke et al., 2022; Qingzu et al., 2019; Yang et al., 2018; Zhang et al., 2007), and detailed explanations and formulas are shown in Supplementary Table S1. The temperature and humidity of the natural factors were measured using a wearable monitoring equipment. The boiler spatial distribution data in the human activity factor were obtained from the latest emission inventory issued by the government of Shenyang City, Liaoning Province. All points were spatially interpolated using different functions (heating and non-heating) to obtain the steam volume and distribution density of the boilers in different seasons in the study area. Other human activity factors were obtained from POI data, which were collected from the 2019 AutoNavi map; there were 13 categories: bank, company, restaurant, facility, government, hospital,

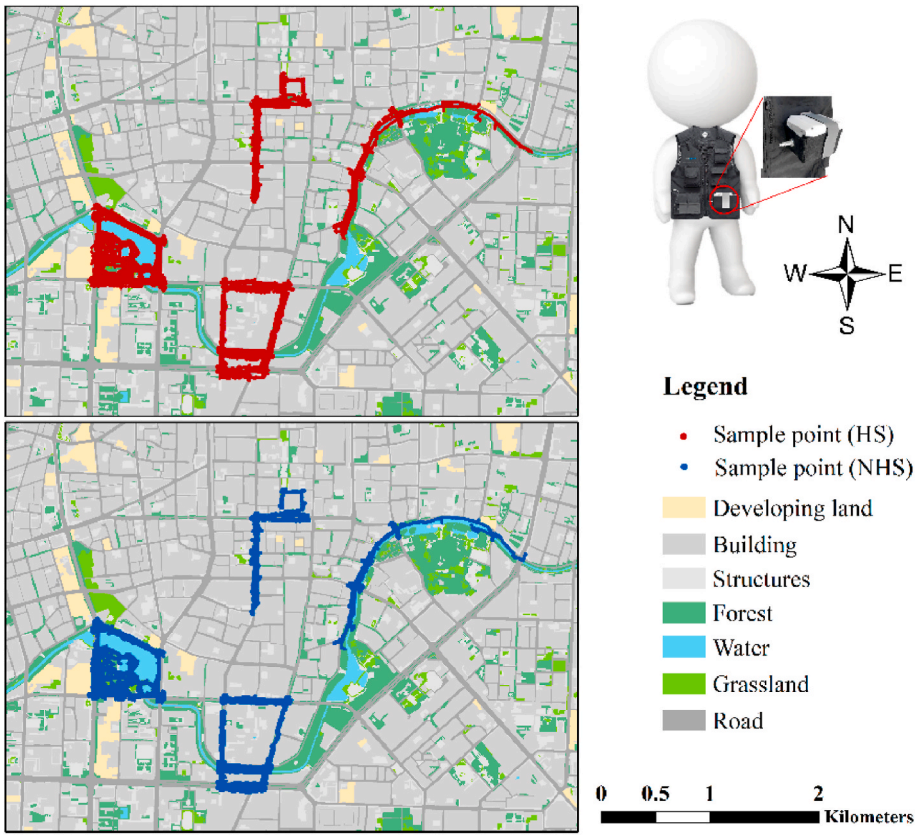

Fig. 1. Air pollution monitoring route map of study area. HS: heating season; NHS: non-heating season. The top right graphic illustrates where a volunteer wears the monitoring equipment.

Table 1
Classification and detailed description of impact factors.

Category	Metrics	Abbreviation	Category	Metrics	Abbreviation
Natural factor	Temperature	TEM	2D landscape pattern index	Percentage of forest area	PLF
	Relative humidity	HUM		Percentage of grassland area	PLG
Human activity factor	Boiler distribution density	BDD		Percentage of developing land area	PLD
	Boiler steam volume	BSV		Percentage of road area	PLR
	Bank	BANK		Percentage of structures area	PLS
	Company	COMP		Percentage of building area	PLB
	Restaurant	REST		Percentage of water area	PLW
	Public facility	FAC		Road area	ROAD
	Government	GOV		Shannon's diversity index	SHDI
	Hospital	HOS		Contagion index	CONTAG
	Hotel	HOTEL	3D landscape pattern index	Aspect	ASP
	Leisure facility	LES		Floor area ratio	FAR
	Living service	LVS		Street valley height to width	H/a
	School	SCH		Highest landscape indices	HLI
	Shopping mall	SHO		Landscape height coefficient of variance	LHCV
	Tourist	TOU		Landscape height density	LHD
	Traffic facility	TRA		Landscape height range	LHR
				Landscape height standard deviation	LHSD
				Landscape otherness	LO
				Landscape volume density	LVD

hotel, leisure, living service, school, shopping, tourist, and traffic. 2D landscape pattern indices were calculated using land use data (Fig. 1) derived from 2019 Geographic Country Data. 3D landscape pattern indices were calculated using building height data from Baidu Map (www.map.baidu.com/), which includes building footprints and building heights (m), with a total average building height deviation of 1.02 m and an accuracy of 86.78% (Liu et al., 2021b). Detailed formulas for the 2D and 3D landscape pattern indices were provided by previous studies (Qingzu et al., 2019; Tian et al., 2019; Uuemaa et al., 2005). Details for each factor are presented in Table 1.

2.3. Data processing and analysis

Extreme values of the monitoring data, where residuals were larger than three times the standard deviation, were removed during the preprocessing stage. To further serve the study, the monitored data during sampling were divided into a grid (50 m), and the mean values were calculated and assigned to each grid. Within each grid, the values of the human activity factors were calculated separately for the factors mentioned in Table 1. To calculate the landscape pattern indices, land use data in vector format within each grid were converted to raster format for importing into Fragstats v4.2.1. All values of the calculated indices were assigned to the corresponding grids to obtain the panel data. Then, we constructed independent RF models and identified significant variables for the two seasons for the three UPM pollutants using panel data. Random forest model fitting was implemented using the random forest package of the R language (Bischl et al., 2016; Zhang et al., 2018). The RF model collects results from randomly selected features from each decision classification tree and aggregates the results from a large number of decision trees. An increase in node purity (IncNodePurity) was used to analyze the importance of each influencing factor in the model (Liu et al., 2021a). Node purity is measured by the sum of squared residuals, and represents the effect of each variable on the heterogeneity of observations at each node of the classification tree, thus comparing the importance of the variables. A higher value of IncNodePurity indicates greater importance of the variable.

Therefore, we used the RF model to assess the relationship between UPM concentrations and the 37 impact factors for different pollutant types in different seasons. Subsequently, model interpretation rates and 10-fold cross-validation were calculated using the random forest package of the R language to assess the accuracy of each model (Bischl et al., 2016). The importance of the impact factors was measured using IncNodePurity. To reveal the importance of significant impact factors on the concentration of UPMs during HS and NHS, we performed a 10-fold cross-validation using the RF model and extracted significant impact factors in combination with IncNodePurity. Specifically, 10-fold cross-validation divides the dataset into ten parts, nine of which are used as training data and one as test data for the experiment. This procedure was independently repeated 10 times to avoid the introduction of any bias when randomly partitioning the dataset in the cross-validation (Zhang et al., 2011). In the RF model, the relationships between UPM concentrations and these factors were investigated by marginal effects analysis, which was implemented in R using the random forest package (Bobbia et al., 2011; Jun, 2021; Li et al., 2020).

3. Results

3.1. Air pollution concentration and model accuracy verification

A total of 222,729 data points (79 days) from the HS and 190,156 data points (122 days) from the NHS were sampled in this study. Table 2 lists the statistical values for the monitored pollutants. PM_{10} had the highest of all indicators in both the HS and NHS, and PM_1 had the lowest. The mean values of the three UPM concentrations were higher in HS than in NHS, and the standard deviation (SD) values were lower in NHS than in NS. These results indicate that HS suffer from more severe air pollution, along with more extreme pollution conditions.

By averaging the UPM monitored by volunteers during HS and NHS, this study found that the concentration of UPM in the two seasons had different spatial-temporal distribution characteristics (Fig. 2). As the diameter of the particulate matter increased, the pollutant concentration increased during both seasons. The spatial distributions of the three UPM types of particulate matter in the same season were similar. For descriptive purposes, this study divided the sampling route into four routes (a, b, c, and d; Fig. 2). The UPM concentration in route a showed high in the external area and low in the internal area in HS and northwest high and southeast low in NHS. The spatial distribution of the UPM along route b was the same in both seasons, with high values in the north

Table 2
Monitoring concentration ($\mu g/m^3$) statistics for UPMs.

	Type	MIN	MAX	MEAN	SD
HS	PM_1	0.00	333.00	38.80	34.23
	$PM_{2.5}$	0.00	758.00	70.28	68.81
	PM_{10}	1.00	951.00	87.48	87.30
NHS	PM_1	0.00	422.00	19.41	18.69
	$PM_{2.5}$	0.00	718.00	29.96	30.38
	PM_{10}	0.00	760.00	34.42	33.50

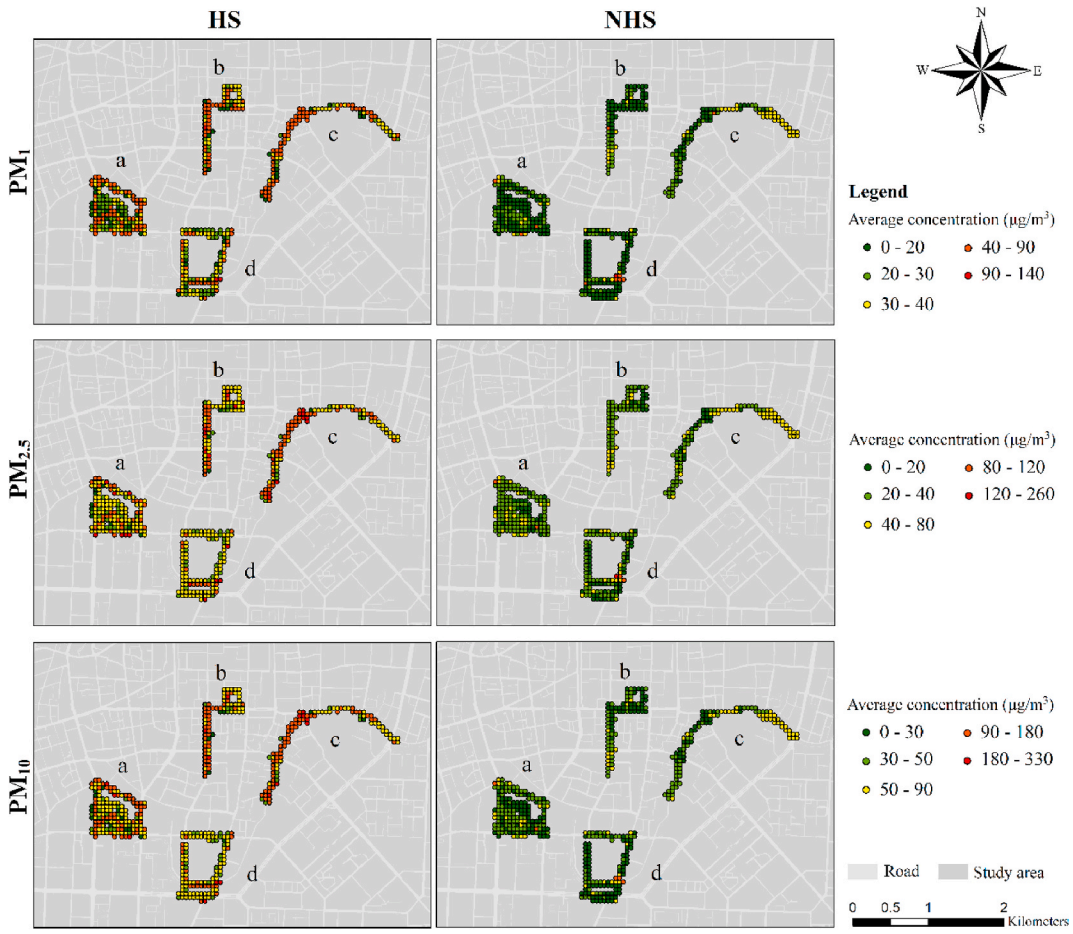

Fig. 2. Average sampling concentrations of PM_1, $PM_{2.5}$ and PM_{10}. HS: heating season; NHS: non-heating season.

and low values in the south. Route c showed high UPM concentrations in the west and low concentrations in the east, but the opposite was true for NHS. The southeast of route d had high concentrations of UPM aggregates in both seasons.

Accuracy was verified for the six random forest models established for the three UPMs in the two seasons. Six models explained 80–90% of the relationship between UPM and the impact factors (Table 3). With an increase in UPM diameter, the interpretation rates of both the HS and NHS models increased. The model's accuracy was similar for $PM_{2.5}$, and PM_{10}, while the accuracy of the $PM_{1.0}$ model was at least 0.6% lower. Overall, the accuracy of all models was greater than 80%. Although the amount of data in the HS model (12,973) was lower than that of the NHS (14,713) after averaging to the grid, the interpretation rate of the former was always higher than that of the latter.

We performed 10-fold cross-validation of the six models (Fig. 3). The cross-validation error of each model decreased sharply and stabilized when the important classes were greater than or equal to nine. The smallest cross-validation error was obtained when nine important classes were used in the HS and 18 important classes were used in the NHS. This indicates that certain influencing factors had a greater impact on the concentration of UPMs in the HS. The model cross-validation error was stable when 9–18 significant classes were used.

Table 3
Interpretation rate of the random forest model.

Type	HS	NHS
$PM_{1.0}$	87.39%	80.2%
$PM_{2.5}$	88.1%	80.81%
PM_{10}	88.49%	80.86%

3.2. *Importance of influencing factors*

IncNodePurity was used to analyze the importance of each influencing factor in the six models. A higher value of IncNodePurity indicates greater importance of the variable. The results are shown in Fig. 4. Natural factors (temperature and humidity) were the most important in all six models, and environmental variables were more important in the HS model than in the NHS model. Apart from the natural factors, boiler distribution density (BDD) and boiler steam volume (BSV) were the most significant artificial factors affecting pollutant concentrations, and the importance of these two factors was slightly higher than that of the other factors in the HS. Percentage of grassland area and Landscape height density (LHD) had a higher impact on the three UPMs in the HS but had less impact on the NHS. Among the six models, shopping mall, tourist, traffic facility, hotel, and percentage of developing land area had the lowest importance.

Fig. 5 shows a stacked Nightingale Rose diagram which illustrates the importance ranking of the factors influencing pollutant concentrations, which can be divided into four levels. Temperature (TEM) and relative humidity (HUM) ranked first with BDD and BSV being in the second rank, indicating that boiler use was the most important artificial factor affecting pollutant concentrations during any season. Most landscape pattern factors rank third. Percentage of forest area has the highest influence on the three UPM concentrations in the HS, followed by Shannon's diversity index (SHDI). The POIs with the least importance are ranked fourth. The importance of each variable increases with particle size. For the model of PM_1, the importance of percentage of water area was higher than that of the other factors, but this was not reflected in the models of the other two pollutants. In both models, percentage of

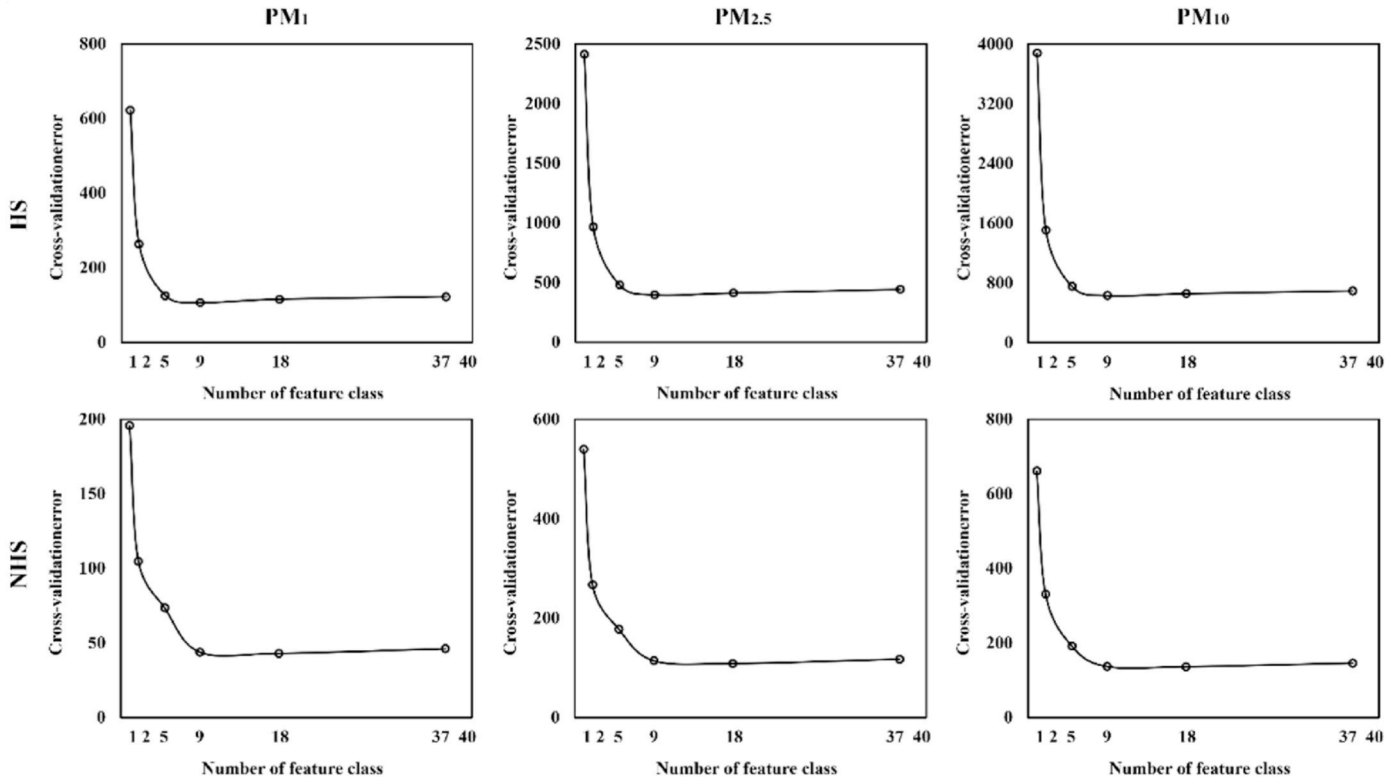

Fig. 3. 10-fold cross-validation of six models.

building area and percentage of forest area (PLF) were more important than PLW. SHDI showed higher importance in the PM_1 and $PM_{2.5}$ models but was not reflected in PM_{10}. This indicates that different landscape patterns have different impacts on different UPMs.

3.3. Marginal effects of influencing factors

Based on the importance of the impact factors calculated by the RF model and the results of the 10-fold cross-validation, 14 impact factors were selected for the marginal effects analysis (Fig. 6). In general, the marginal effect of each influencing factor on UPM increased with diameter of the UPM, with HS changing more dramatically than NHS. The effect of TEM on UPM concentration tended to decrease and then increase, with the lowest effect on UPM concentration at 25 °C (NHS) and 3 °C (HS). This oscillation was due to the exceptionally high levels of UPM generated by central heating in the study area during winter when the atmospheric quasi-stationary fronts hinder the transport and diffusion of UPM. The effect of HUM on UPM concentration increased rapidly with increasing HUM, especially in HS, because high HUM contributes to UPM condensation. The effect of BDD on UPM concentration varied considerably in different seasons. Its effect on UPM increased sharply in HS when the BDD reached 6, which indicated that central heating boilers are the major cause of air pollution in the study area. As BSV increased, it had a large, stabilizing effect on the concentration of UPM in the HS. Regardless of the BSV, boilers can cause considerable pollution once they are in operation.

The effect of PLF steady increased by 75% (HS) and 25% (NHS), whereas the overall change in PLW was flat because of the low percentage of these two land types in the study area. The impact of the SHDI on UPM reaches a minimum of approximately one (1) in the HS, but the changes are flat in the NHS, which suggests that an appropriately complex mix of land types can reduce the impact on UPM. Compared with other 3D landscape pattern indices, the marginal effect increased sharply when the landscape height range reached 100 in the HS. Thus, low-rise built-up areas had less effect on UPM concentrations than single tall buildings. The effects of street valley height to width (H/a) and LHD on UPM showed a similar slow increase, with dense and tall buildings hindering pollutant dispersion when large amounts of pollutants enter such spaces. The effects of floor area ratio and landscape volume density were lowest at 1.3 and 5, respectively, so, for this factor, tall buildings or low-built-up areas had the least effect on the dispersion of UPM. The effect of landscape height standard deviation (LHSD) remained stable after a slow increase to 50, indicating that the vertical differences in the surface landscape reached their maximum impact on the ability to disperse pollutants at a certain level. Simple surface morphology thus facilitates the dispersion of UPM.

4. Discussion

4.1. Importance of influencing factors under different models

The RF model was used to perform an importance analysis of the factors influencing UPM. In this study, we included a more comprehensive set of influencing factors, and the results suggest that the RF model is highly applicable in analyzing the importance of complex influencing factors on UPM. Among the 37 influencing factors, TEM and HUM were the most important. This is the same conclusion reached in previous studies that used different models (Gao et al., 2011; Li et al., 2017). However, a greater effect of TEM and HUM on air pollution during HS was found in this study, distinguishing between HS and NHS. Unique climatic conditions can exacerbate air pollution events during HS (Huang et al., 2015). Industrial production and residential heating boilers are the primary artificial factors causing air pollution, especially $PM_{2.5}$, and PM_{10} in HS. This is because the combination of unfavorable meteorological conditions and energy consumption due to central heating in northern China causes frequent air pollution (Lin and Ling, 2021; Shi et al., 2020). Previous studies have shown that the spatial allocation of urban buildings and green spaces and the combined pattern of buildings of different heights could significantly affect the dispersion of pollutants (Abhijith et al., 2017; Yang et al., 2020). However, our

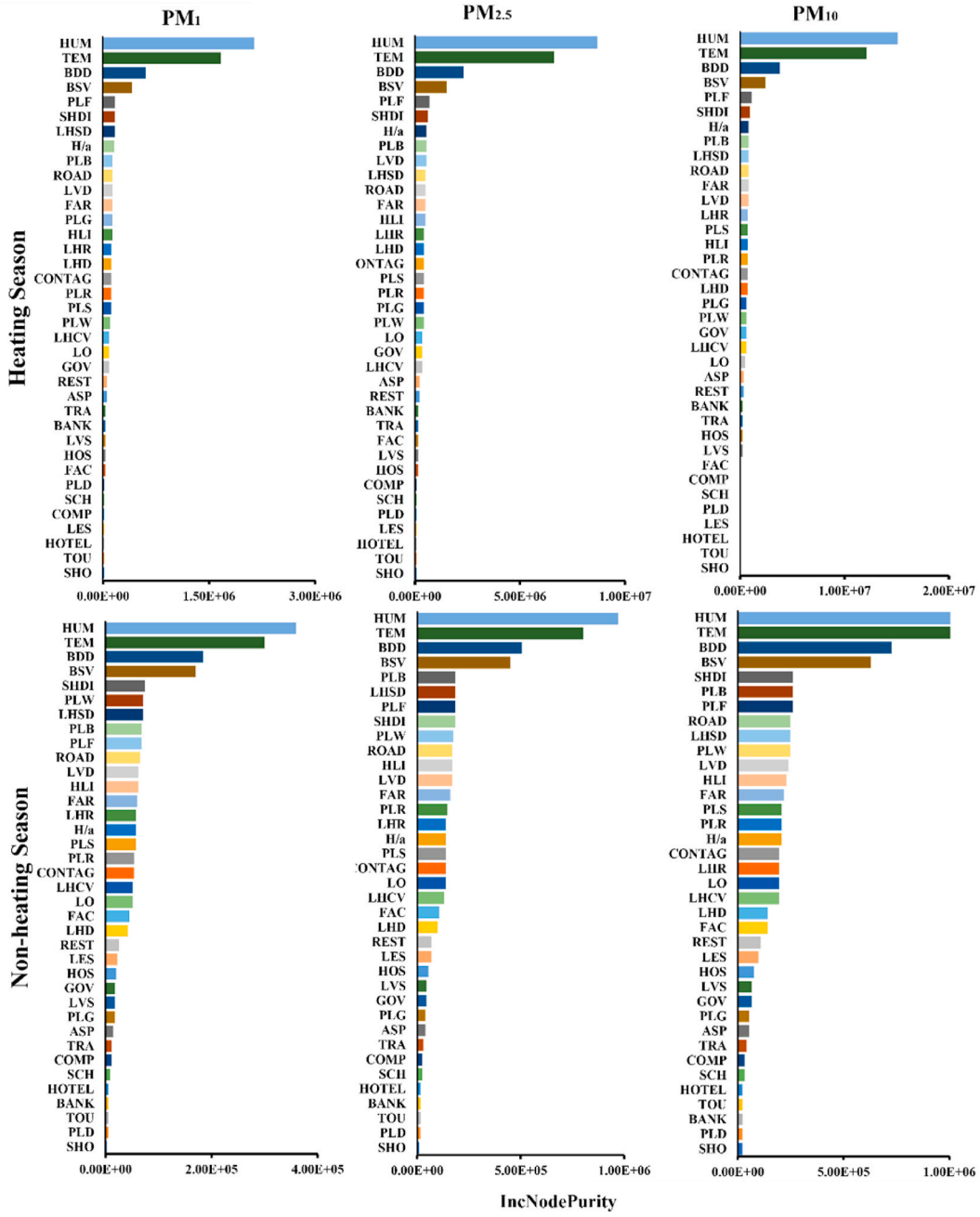

Fig. 4. IncNodePurity of each impact factor under the six models. TEM: temperature; HUM: relative humidity; BDD: boiler distribution density; BSV: boiler steam volume; BANK: bank; COMP: company; REST: restaurant; FAC: public facility; GOV: government; HOS: hospital; HOTEL: hotel; LES: leisure facility; LVS: living service; SCH: school; SHO: shopping mall; TOU: tourist; TRA: traffic facility; PLF: percentage of forest area; PLG: percentage of grassland area; PLD: percentage of developing land area; PLB: percentage of building area; PLS: percentage of structures area; PLR: percentage of road area; PLW: percentage of water area; ROAD: road area; SHDI: Shannon's diversity index; CONTAG: contagion index; ASP: aspect; FAR: floor area ratio; H/a: street valley height to width; HLI: highest landscape indices; LHCV: landscape height coefficient of variance; LHD: landscape height density; LHR: landscape height range; LHSD: landscape height standard deviation; LO: landscape otherness; LVD: landscape volume density.

study further found that for urban landscape patterns, PLF, SHDI, H/a, PLB, and LHSD are important influences on the concentration of each pollutant during HS and NHS, but NHS requires more major factors to influence UPM.

4.2. Marginal effects of the main factors on the UPM concentration

The marginal effects method for the RF model was used to quantitatively analyze the main factors. Some studies have been conducted to quantitatively analyze the relationship between UPM and various influencing factors using marginal effects methods from other models (Li et al., 2020). The results of our study enrich the available models for existing marginal effects analysis. The lower the TEM of the HS, the greater its effect on UPM concentration, which may be because more energy consumption at lower temperatures leads to more pollution emissions (Luo and Xia, 2020). The effect also increased when the temperature rose above 3 °C. This is because of the formation of quasi-stationary fronts by equally matched warm and cold air masses that stop the spread of UPM (Huang et al., 2015). Owing to the limited distance of heat transfer, heating boilers are often located in dense

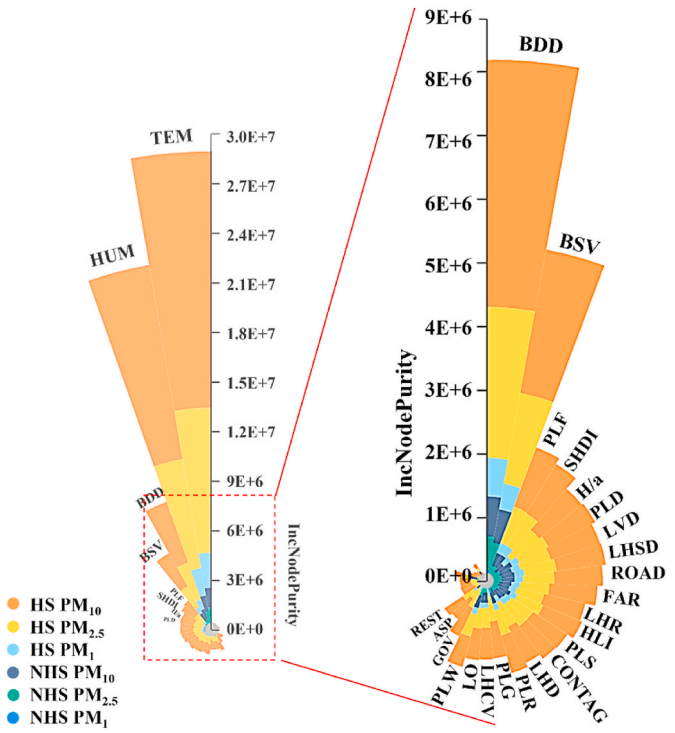

Fig. 5. Stacked Nightingale Rose diagram of the importance ranking of factors under the six models. TEM: temperature; HUM: relative humidity; BDD: boiler distribution density; BSV: boiler steam volume; BANK: bank; COMP: company; REST: restaurant; FAC: public facility; GOV: government; HOS: hospital; HOTEL: hotel; LES: leisure facility; LVS: living service; SCH: school; SHO: shopping mall; TOU: tourist; TRA: traffic facility; PLF: percentage of forest area; PLG: percentage of grassland area; PLD: percentage of developing land area; PLB: percentage of building area; PLS: percentage of structures area; PLR: percentage of road area; PLW: percentage of water area; ROAD: road area; SHDI: Shannon's diversity index; CONTAG: contagion index; ASP: aspect; FAR: floor area ratio; H/a: street valley height to width; HLI: highest landscape indices; LHCV: landscape height coefficient of variance; LHD: landscape height density; LHR: landscape height range; LHSD: landscape height standard deviation; LO: landscape otherness; LVD: landscape volume density.

built-up urban areas (Kauko et al., 2020; Xu et al., 2014). Therefore, it is disadvantageous to diffuse UPM during winter (Su et al., 2018). However, this study found that once a boiler is put into service, a BDD of 6 or more will have a significant impact on UPM, no matter how large the BSV is, which indicates that compared with dispersed small boilers, a large centrally distributed boiler production system within the city would be more beneficial to the management of UPM. This is also in line with the reform program proposed in China's Blue Sky Plan in recent years (Jiang et al., 2021). The impact of road on UPM in different seasons shows that traffic and residential sources may work collaboratively to aggravate winter haze events in areas with high traffic density(Sun et al., 2013). Previous studies have found that the climate in northern China causes vegetation to have a reduced or even a negative impact on air purification capacity (Setala et al., 2013). Our study further revealed that a rapid change in this impact occurred when the vegetation area reached 75% in HS; otherwise, the change was flat. Simple urban 3D morphology contributes to the diffusion of air pollutants (Abhijith et al., 2017; Yuan et al., 2014). This conclusion is specified in our results, as single high-rise buildings or low-rise building blocks have the least effect on the transport and diffusion of UPM.

4.3. Strength and limitations

Compared with previous studies, the wearable monitoring equipment used in this study has higher flexibility than vehicle and fixed monitoring, and more realistically reflects the exposure of urban residents to UPM. The collected Sniffer4D data have high spatial-temporal resolution and are thus more helpful in addressing research issues at fine scales and in complex conditions in urban areas. The long-term pollutant monitoring data we obtained, which had high spatial-temporal resolution, will further be used for comparative analysis at finer spatial-temporal scales (e.g., weekdays and weekends, residential and commercial areas) in our subsequent studies. Our study selected multiple influencing factors to consider the effects of nature, human activities, and urban patterns on UPM. This combination of factors makes it easier to identify the impacts of complex effects. Multisource big data applications can provide greater detail on urban air pollution. This study distinguishes between the heating and non-heating seasons, finding that factors have different effects in these two seasons, which is a more useful analysis of UPM influencing factors in centrally heated areas than in previous studies. Owing to the difficulty of quantitatively analyzing urban environmental studies, our study makes a preliminary attempt to use the marginal effects of the RF model. The results showed that marginal effects analysis can quantitatively identify the relationship between urban patterns and air pollution diffusion processes.

The Sniffer4D low-cost monitoring device used in this study is based on the light-scattering principle for collection of UPM concentrations. Compared to traditional gravimetric analysis for particulate matter monitoring, this method has difficulty distinguishing water droplets from particulate matter, and therefore cannot achieve the same high accuracy (Lee et al., 2020). Improving the accuracy is one of the main goals of the development of low-cost transmission monitoring equipment. Although this study developed a detailed wearable device monitoring process based on different seasons, the spatial distribution of air pollutants showed significant day and night differences (Ma et al., 2020a). However, nighttime changes in UPM were not monitored in our study, so it was not possible to compare with the daytime results. Adding nighttime monitoring in a subsequent study will facilitate the investigation of the effects of different resident activity patterns on UPM. RF models act like black boxes with no control over the inner workings, and may overfit the data modeled by certain factors (Breiman, 2001). In addition, the accuracy of our RF model was lower in the non-heating season, so the factors affecting this need to be further investigated. In our study, road density was selected to assess traffic flow; however, these estimates may have caused some inaccuracies. To match long-term pollution monitoring data, big data platforms should be used to incorporate more detailed traffic data (Fedorov et al., 2019). At the same time, the impact of seasonal changes on water bodies or woodland meadows should be considered to further refine the processing of impact factors (Hoppa et al., 2022; Setala et al., 2013). Our study did not investigate factors such as wind speed and corridors because of the limitations of the monitoring equipment. These are also important natural factors that must be explored. In the future, more integrated equipment is required to collect and analyze these important natural factors. In addition, although we mentioned that temperature and humidity are the primary and most important factors influencing the change in UPM concentration, urban temperature is also influenced by the heat island phenomenon (Xu et al., 2018). Therefore, combining the effects of human activities on the heat island phenomenon and UPM transport and diffusion requires further investigation.

5. Conclusions

In this study, near-surface UPM pollutant (PM_1, $PM_{2.5}$ and PM_{10}) concentrations were collected for one year during two time periods (HS and NHS) in the Shenyang urban areas using wearable monitoring equipment. This monitoring method provides a more realistic indication of residents' exposure to UPM. The monitoring results showed that heavy weather conditions were more frequent in HS. Furthermore, the importance of the 37 selected influencing factors on the UPM concentration was assessed using the IncNodePurity of the RF model. Among

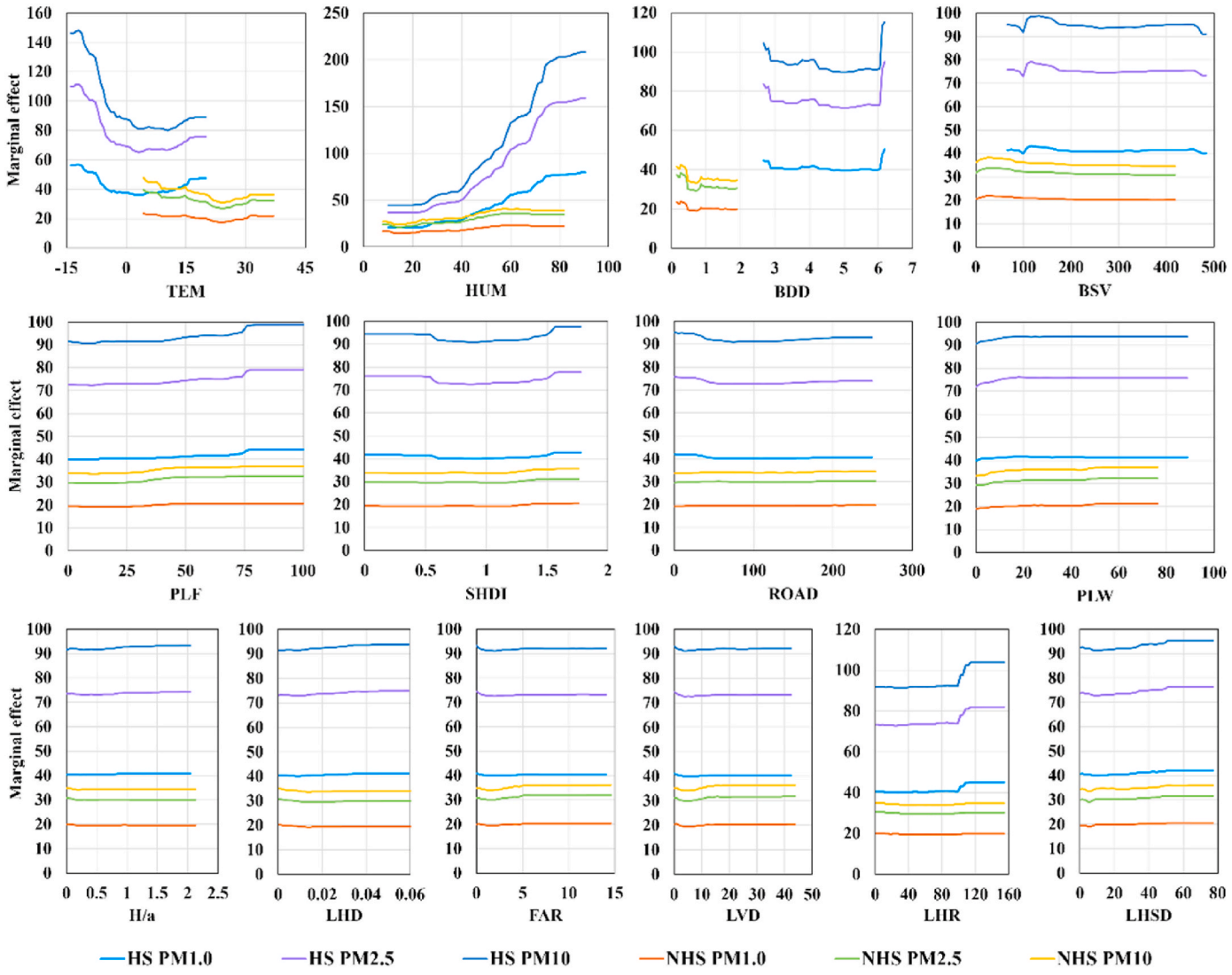

Fig. 6. The marginal effects of the main factor changes on the UPM concentration. TEM: temperature; HUM: relative humidity; BDD: boiler distribution density; BSV: boiler steam volume; PLF: percentage of forest area; PLW: percentage of water area; ROAD: road area; SHDI: Shannon's diversity index; FAR: floor area ratio; H/a: street valley height to width; LHD: landscape height density; LHR: landscape height range; LHSD: landscape height standard deviation; LVD: landscape volume density.

them, temperature and humidity play a decisive role, but the central heating boiler is the main factor that causes UPM concentration to exhibit variations in the two seasons. This study, which distinguishes HS and NHS within the city, can provide a more realistic response to the causal factors of transmission diffusion generated by UPM. The marginal effects of the important influencing factors were analyzed after 10-fold cross-validation and IncNodePurity analysis. The results showed that large individual boilers were more beneficial for UPM prevention and control than small dispersed boilers. Increasing land type diversity while retaining a large area of water and forests is beneficial for reducing UPM concentrations. Simpler 3D patterns, such as low-building groups or tall single buildings, are more beneficial for UPM dispersion than tall building groups. This quantitative study will be helpful towards understanding and improving urban ecology. By integrating and analyzing multiple sources of big data, this study offers scientific recommendations for optimal land use configuration to address urban air pollution within the urban planning field.

Author contributions

Chuyi Zhang: Conceptualization, Methodology, Formal analysis, Investigation, Writing - Original Draft; Yuanman Hu: Methodology, Project administration; Matthew D. Adams: Writing - Review & Editing; Miao Liu: Investigation, Resources; Binglun Li, Tuo Shi: Software; Chunlin Li: Methodology, Writing - Review & Editing.

Declaration of competing interest

The authors declare the following financial interests/personal relationships which may be considered as potential competing interests:

Data availability

The authors do not have permission to share data.

Acknowledgments

This study was financially supported by the National Natural Science Foundation of China (Nos. 41730647, 41671184, 41671185, and 41871192). Chuyi Zhang thanks the China Scholarship Council (No. 202004910511) for fellowship support.

Appendix A. Supplementary data

Supplementary data to this article can be found online at https://doi.org/10.1016/j.envres.2022.114393.

References

Abhijith, K.V., Kumar, P., Gallagher, J., McNabola, A., Baldauf, R., Pilla, F., Broderick, B., Di Sabatino, S., Pulvirenti, B., 2017. Air pollution abatement performances of green infrastructure in open road and built-up street canyon environments - a review. Atmos. Environ. 162, 71–86.

Administration, C.M., 2021. Atmospheric Environmental Weather Bulletin, 2020.

Althuwaynee, O.F., Balogun, A.L., Al Madhoun, W., 2020. Air pollution hazard assessment using decision tree algorithms and bivariate probability cluster polar function: evaluating inter-correlation clusters of PM10 and other air pollutants. GIScience Remote Sens. 57, 207–226.

An, Z.S., Huang, R.J., Zhang, R.Y., Tie, X.X., Li, G.H., Cao, J.J., Zhou, W.J., Shi, Z.G., Han, Y.M., Gu, Z.L., Ji, Y.M., 2019. Severe haze in northern China: a synergy of anthropogenic emissions and atmospheric processes. Proc. Natl. Acad. Sci. U.S.A. 116, 8657–8666.

Azarmi, F., Kumar, P., Marsh, D., Fuller, G., 2016. Assessment of the long-term impacts of PM10 and PM2.5 particles from construction works on surrounding areas. Environ. Sci.-Processes Impacts 18, 208–221.

Bischl, B., Lang, M., Kotthoff, L., Schiffner, J., Richter, J., Studerus, E., Casalicchio, G., Jones, Z.M., 2016. Machine learning in R. J. Mach. Learn. Res. 17.

Bobbia, M., Jollois, F.X., Poggi, J.M., Portier, B., 2011. Quantifying local and background contributions to PM10 concentrations in Haute-Normandie, using random forests. Environmetrics 22, 758–768.

Breiman, L., 2001. Random forests. Mach. Learn. 45, 5–32.

Bulot, F.M.J., Johnston, S.J., Basford, P.J., Easton, N.H.C., Apetroaie-Cristea, M., Foster, G.L., Morris, A.K.R., Cox, S.J., Loxham, M., 2019. Long-term field comparison of multiple low-cost particulate matter sensors in an outdoor urban environment. Sci. Rep. 9.

Cao, T.T., Thompson, J.E., 2017. Portable, ambient PM2.5 sensor for human and/or animal exposure studies. Anal. Lett. 50, 712–723.

Castell, N., Dauge, F.R., Schneider, P., Vogt, M., Lerner, U., Fishbain, B., Broday, D., Bartonova, A., 2017. Can commercial low-cost sensor platforms contribute to air quality monitoring and exposure estimates? Environ. Int. 99, 293–302.

Chang, Q., Zhang, H.H., Zhao, Y.H., 2020. Ambient air pollution and daily hospital admissions for respiratory system-related diseases in a heavy polluted city in Northeast China. Environ. Sci. Pollut. Control Ser. 27, 10055–10064.

Chen, L.D., Fu, B.J., Zhao, W.W., 2006. Source-sink landscape theory and its ecological significance. Acta Ecol. Sin. 26 (5), 1444–1449.

Chen, C.R., Zhang, H.X., Yan, W.J., Wu, N.A., Zhang, Q., He, K.B., 2021. Aerosol water content enhancement leads to changes in the major formation mechanisms of nitrate and secondary organic aerosols in winter over the North China Plain. Environ. Pollut. 287.

Chen, F.L., Chen, Z.F., 2021. Cost of Economic Growth: Air Pollution and Health Expenditure. Science of the Total Environment, p. 755.

China, N.B.o.S.o., 2020. Statistical communique on national economic and social development of the people's Republic of China 2020. China Popul. Today 33, 22–42.

Choi, W., Ranasinghe, D., DeShazo, J.R., Kim, J.J., Paulson, S.E., 2018. Where to locate transit stops: cross-intersection profiles of ultrafine particles and implications for pedestrian exposure. Environ. Pollut. 233, 235–245.

Fedorov, A., Nikolskaia, K., Ivanov, S., Shepelev, V., Minbaleev, A., 2019. Traffic flow estimation with data from a video surveillance camera. Journal of Big Data 6.

Gao, H.W., Chen, J., Wang, B., Tan, S.C., Lee, C.M., Yao, X.H., Yan, H., Shi, J.H., 2011. A study of air pollution of city clusters. Atmos. Environ. 45, 3069–3077.

Gao, J.H., Woodward, A., Vardoulakis, S., Kovats, S., Wilkinson, P., Li, L.P., Xu, L., Li, J., Yang, J., Li, J., Cao, L., Liu, X.B., Wu, H.X., Liu, Q.Y., 2017a. Haze, public health and mitigation measures in China: a review of the current evidence for further policy response. Sci. Total Environ. 578, 148–157.

Gao, S., Janowicz, K., Couclelis, H., 2017b. Extracting urban functional regions from points of interest and human activities on location-based social networks. Trans. GIS 21, 446–467.

Greenstone, M., He, G., Jia, R., Liu, T., 2022. Can technology solve the principal-agent problem? Evidence from China's war on air pollution. American Economic Review-Insights 4, 54–70.

Guo, B.L., Zhou, K.B., Sun, Y., Ma, K.R., 2021. Study on the characteristics and trends of spatial and temporal changes of air quality in Northeast China. Resources Economization & Environmental 20–23.

Helbig, C., Ueberham, M., Becker, A.M., Marquart, H., Schlink, U., 2021. Wearable sensors for human environmental exposure in urban settings. Current Pollution Reports 7, 417–433.

Hoppa, A., Sikorska, D., Przybysz, A., Melon, M., Sikorski, P., 2022. The role of trees in winter air purification on children's routes to school. Forests 13.

Hu, X.F., Belle, J.H., Meng, X., Wildani, A., Waller, L.A., Strickland, M.J., Liu, Y., 2017. Estimating PM2.5 concentrations in the conterminous United States using the random forest approach. Environ. Sci. Technol. 51, 6936–6944.

Huang, P., Zhang, J.Y., Tang, Y.X., Liu, L., 2015. Spatial and temporal distribution of PM2.5 pollution in xi'an city, China. Int. J. Environ. Res. Publ. Health 12, 6608–6625.

Jiang, X., Li, G.L., Fu, W., 2021. Government environmental governance, structural adjustment and air quality: a quasi-natural experiment based on the Three-year Action Plan to Win the Blue Sky Defense War. J. Environ. Manag. 277.

Jovasevic-Stojanovic, M., Bartonova, A., Topalovic, D., Lazovic, I., Pokric, B., Ristovski, Z., 2015. On the use of small and cheaper sensors and devices for indicative citizen-based monitoring of respirable particulate matter. Environ. Pollut. 206, 696–704.

Jun, M.J., 2021. A comparison of a gradient boosting decision tree, random forests, and artificial neural networks to model urban land use changes: the case of the Seoul metropolitan area. Int. J. Geogr. Inf. Sci. 35, 2149–2167.

Karagulian, F., Barbiere, M., Kotsev, A., Spinelle, L., Gerboles, M., Lagler, F., Redon, N., Crunaire, S., Borowiak, A., 2019. Review of the performance of low-cost sensors for air quality monitoring. Atmosphere 10.

Karagulian, F., Belis, C.A., Dora, C.F.C., Pruss-Ustun, A.M., Bonjour, S., Adair-Rohani, H., Amann, M., 2015. Contributions to cities' ambient particulate matter (PM): a systematic review of local source contributions at global level. Atmos. Environ. 120, 475–483.

Kauko, H., Rohde, D., Hafner, A., 2020. Local heating networks with waste heat utilization: low or medium temperature supply? Energies 13.

Ke, B., Hu, W.H., Huang, D.M., Zhang, J., Lin, X.T., Li, C.H., Jin, X.J., Chen, J., 2022. Three-dimensional Building Morphology Impacts on PM2.5 Distribution in Urban Landscape Settings in Zhejiang, China. Science of the Total Environment, p. 826.

Khomenko, S., Cirach, M., Pereira-Barboza, E., Mueller, N., Barrera-Gomez, J., Rojas-Rueda, D., Hoogh, K.D., Hoek, G., Nieuwenhuijsen, M., 2021. Premature mortality due to air pollution in European cities: a health impact assessment. Lancet Planet. Health 5, E121–E134.

Kim, K.H., Kabir, E., Kabir, S., 2015. A review on the human health impact of airborne particulate matter. Environ. Int. 74, 136–143.

Kumar, P., Morawska, L., Martani, C., Biskos, G., Neophytou, M., Di Sabatino, S., Bell, M., Norford, L., Britter, R., 2015. The rise of low-cost sensing for managing air pollution in cities. Environ. Int. 75, 199–205.

Lee, H., Kang, J., Kim, S., Im, Y., Yoo, S., Lee, D., 2020. Long-term evaluation and calibration of low-cost particulate matter (PM) sensor. Sensors 20.

Li, C.L., Liu, M., Hu, Y.M., Zhou, R., Huang, N., Wu, W., Liu, C., 2020. Spatial Distribution Characteristics of Gaseous Pollutants and Particulate Matter inside a City in the Heating Season of Northeast China. Sustainable Cities and Society, p. 61.

Li, J.D., Liao, H., Hu, J.L., Li, N., 2019. Severe particulate pollution days in China during 2013-2018 and the associated typical weather patterns in Beijing-Tianjin-Hebei and the Yangtze River Delta regions. Environ. Pollut. 248, 74–81.

Li, Q., Wang, E.R., Zhang, T.T., Hu, H., 2017. Spatial and temporal patterns of air pollution in Chinese cities. Water Air Soil Pollut. 228.

Lin, B.Q., Ling, C.X., 2021. Heating price control and air pollution in China: evidence from heating daily data in autumn and winter. Energy Build. 250.

Liu, J., Kiesewetter, G., Klimont, Z., Cofala, J., Heyes, C., Schopp, W., Zhu, T., Cao, G.Y., Sanabria, A.G., Sander, R., Guo, F., Zhang, Q., Nguyen, B., Bertok, I., Rafaj, P., Amann, M., 2019. Mitigation pathways of air pollution from residential emissions in the Beijing-Tianjin-Hebei region in China. Environ. Int. 125, 236–244.

Liu, J., Mauzerall, D.L., Chen, Q., Zhang, Q., Song, Y., Peng, W., Klimont, Z., Qiu, X.H., Zhang, S.Q., Hu, M., Lin, W.L., Smith, K.R., Zhu, T., 2016. Air pollutant emissions from Chinese households: a major and underappreciated ambient pollution source. Proc. Natl. Acad. Sci. U.S.A. 113, 7756–7761.

Liu, J.J., Zhou, T., Luo, H., Liu, X., Yu, P.X., Zhang, Y.J., Zhou, P.F., 2021a. Diverse roles of previous years' water conditions in gross primary productivity in China. Rem. Sens. 13.

Liu, M., Ma, J., Zhou, R., Li, C.L., Li, D.K., Hu, Y.M., 2021b. High-resolution mapping of mainland China's urban floor area. Landsc. Urban Plann. 214.

Lowicki, D., 2019. Landscape pattern as an indicator of urban air pollution of particulate matter in Poland. Ecol. Indicat. 97, 17–24.

Luo, A., Xia, J.J., 2020. Policy on energy consumption of district heating in northern China: historical evidence, stages, and measures. J. Clean. Prod. 256.

Ma, J., Tao, Y.H., Kwan, M.P., Chai, Y.W., 2020a. Assessing mobility-based real-time air pollution exposure in space and time using smart sensors and GPS trajectories in beijing. Ann. Assoc. Am. Geogr. 110, 434–448.

Ma, R.M., Ban, J., Wang, Q., Li, T.T., 2020b. Statistical Spatial-Temporal Modeling of Ambient Ozone Exposure for Environmental Epidemiology Studies: A Review. Science of the Total Environment, p. 701.

Ma, Z., 2021. Characteristic analysis of changes in urban ambient air pollution factors in northeast China during "the 13th five-year plan period. Journal of Green Science and Technology 23, 155–157.

Mahajan, S., Kumar, P., 2020. Evaluation of Low-Cost Sensors for Quantitative Personal Exposure Monitoring, vol. 57. Sustainable Cities and Society.

Mallires, K.R., Wang, D., Tipparaju, V.V., Tao, N.J., 2019. Developing a low-cost wearable personal exposure monitor for studying respiratory diseases using metal-oxide sensors. IEEE Sensor. J. 19, 8252–8261.

McKercher, G.R., Salmond, J.A., Vanos, J.K., 2017. Characteristics and applications of small, portable gaseous air pollution monitors. Environ. Pollut. 223, 102–110.

Miao, C.P., Yu, S., Hu, Y.M., Bu, R.C., Qi, L., He, X.Y., Chen, W., 2020. How the Morphology of Urban Street Canyons Affects Suspended Particulate Matter Concentration at the Pedestrian Level: an In-Situ Investigation, vol. 55. Sustainable Cities and Society.

Morawska, L., Thai, P.K., Liu, X.T., Asumadu-Sakyi, A., Ayoko, G., Bartonova, A., Bedini, A., Chai, F.H., Christensen, B., Dunbabin, M., Gao, J., Hagler, G.S.W., Jayaratne, R., Kumar, P., Lau, A.K.H., Louie, P.K.K., Mazaheri, M., Ning, Z., Motta, N., Mullins, B., Rahman, M.M., Ristovski, Z., Shafiei, M., Tjondronegoro, D., Westerdahl, D., Williams, R., 2018. Applications of low-cost sensing technologies for

air quality monitoring and exposure assessment: how far have they gone? Environ. Int. 116, 286–299.
Pang, N.N., Gao, J., Zhu, G.H., Hui, L.R., Zhao, P.S., Xu, Z.J., Tang, W., Chai, F., 2021. Impact of clean air action on the PM2.5 pollution in Beijing, China: insights gained from two heating seasons measurements. Chemosphere 263.
Pattinson, W., Kingham, S., Longley, I., Salmond, J., 2017. Potential pollution exposure reductions from small-distance bicycle lane separations. J. Transport Health 4, 40–52.
Pope, C.A., Coleman, N., Pond, Z.A., Burnett, R.T., 2020. Fine Particulate Air Pollution and Human Mortality: 25+years of Cohort Studies, vol. 183. Environmental Research.
Qingzu, L., Bo, L., Caihua, Y., Xinshi, Z., Ying, Z., 2019. Preliminary analysis about impacts of urban 3D landscape pattern on regional meteorological condition in Beijng. Ecology and Environmental Sciences 28, 514–522.
Qu, F.F., Liu, F.F., Zhang, H.R., Chao, L.S., Guan, J.T., Li, R.Q., Yu, F.X., Yan, X.X., 2019. Comparison of air pollutant-related hospitalization burden from AECOPD in Shijiazhuang, China, between heating and non-heating season. Environ. Sci. Pollut. Control Ser. 26, 31225–31233.
Rahman, M.S., Islam, A.R.M.T., 2019. Are precipitation concentration and intensity changing in Bangladesh overtimes? Analysis of the possible causes of changes in precipitation systems. Sci. Total Environ. 690, 370–387.
Rai, A.C., Kumar, P., Pilla, F., Skouloudis, A.N., Di Sabatino, S., Ratti, C., Yasar, A., Rickerby, D., 2017. End-user perspective of low-cost sensors for outdoor air pollution monitoring. Sci. Total Environ. 607, 691–705.
Rakowska, A., Wong, K.C., Townsend, T., Chan, K.L., Westerdahl, D., Ng, S., Mocnik, G., Drinovec, L., Ning, Z., 2014. Impact of traffic volume and composition on the air quality and pedestrian exposure in urban street canyon. Atmos. Environ. 98, 260–270.
Rivera, M., Basagana, X., Aguilera, I., Agis, D., Bouso, L., Foraster, M., Medina-Ramon, M., Pey, J., Kunzli, N., Hoek, G., 2012. Spatial distribution of ultrafine particles in urban settings: a land use regression model. Atmos. Environ. 54, 657–666.
Setala, H., Viippola, V., Rantalainen, A.L., Pennanen, A., Yli-Pelkonen, V., 2013. Does urban vegetation mitigate air pollution in northern conditions? Environ. Pollut. 183, 104–112.
Shi, T., Hu, Y.M., Liu, M., Li, C.L., Zhang, C.Y., Liu, C., 2020. Land Use Regression Modelling of PM2.5 Spatial Variations in Different Seasons in Urban Areas. Science of the Total Environment, p. 743.
Shi, Y., Wang, G.L., Gao, X.J., Xu, Y., 2018. Effects of climate and potential policy changes on heating degree days in current heating areas of China. Sci. Rep. 8.
Strobl, C., Boulesteix, A.L., Kneib, T., Augustin, T., Zeileis, A., 2008. Conditional variable importance for random forests. BMC Bioinf. 9.
Su, C., Madani, H., Palm, B., 2018. Heating solutions for residential buildings in China: current status and future outlook. Energy Convers. Manag. 177, 493–510.
Sun, Y.L., Wang, Z.F., Fu, P.Q., Yang, T., Jiang, Q., Dong, H.B., Li, J., Jia, J.J., 2013. Aerosol composition, sources and processes during wintertime in Beijing, China. Atmos. Chem. Phys. 13, 4577–4592.
Tian, Y.Y., Zhou, W.Q., Qian, Y.G., Zheng, Z., Yan, J.L., 2019. The effect of urban 2D and 3D morphology on air temperature in residential neighborhoods. Landsc. Ecol. 34, 1161–1178.
Uuemaa, E., Roosaare, J., Mander, U., 2005. Scale dependence of landscape metrics and their indicatory value for nutrient and organic matter losses from catchments. Ecol. Indicat. 5, 350–369.
Vu, T.V., Shi, Z.B., Cheng, J., Zhang, Q., He, K.B., Wang, S.X., Harrison, R.M., 2019. Assessing the impact of clean air action on air quality trends in Beijing using a machine learning technique. Atmos. Chem. Phys. 19, 11303–11314.
Wang, L., Guan, Q.Y., Wang, F.F., Yang, L.Q., Liu, Z.Y., 2018. Association between heating seasons and criteria air pollutants in three provincial capitals in northern China: spatiotemporal variation and sources contribution. Build. Environ. 132, 233–244.
Wang, S.L., Li, Y.T., Hague, M., 2019. Evidence on the impact of winter heating policy on air pollution and its dynamic changes in north China. Sustainability 11.
Weber, N., Haase, D., Franck, U., 2014. Assessing modelled outdoor traffic-induced noise and air pollution around urban structures using the concept of landscape metrics. Landsc. Urban Plann. 125, 105–116.
Weichenthal, S., Olaniyan, T., Christidis, T., Lavigne, E., Hatzopoulou, M., Van Ryswyk, K., Tjepkema, M., Burnett, R., 2020. Within-city spatial variations in ambient ultrafine particle concentrations and incident brain tumors in adults. Epidemiology 31, 177–183.
Weng, Q.H., Yang, S.H., 2006. Urban air pollution patterns, land use, and thermal landscape: an examination of the linkage using GIS. Environ. Monit. Assess. 117, 463–489.
Wu, J.G., 2013. Landscape sustainability science: ecosystem services and human well-being in changing landscapes. Landsc. Ecol. 28, 999–1023.
Wu, J.G., Hobbs, R., 2002. Key issues and research priorities in landscape ecology: an idiosyncratic synthesis. Landsc. Ecol. 17, 355–365.
Xie, X.Z., Semanjski, I., Gautama, S., Tsiligianni, E., Deligiannis, N., Rajan, R.T., Pasveer, F., Philips, W., 2017. A review of urban air pollution monitoring and exposure assessment methods. ISPRS Int. J. Geo-Inf. 6.
Xu, X., You, S.J., Zheng, X.J., Li, H., 2014. A survey of district heating systems in the heating regions of northern China. Energy 77, 909–925.
Xu, X.Y., Gonzalez, J.E., Shen, S.H., Miao, S.G., Dou, J.X., 2018. Impacts of urbanization and air pollution on building energy demands - beijing case study. Appl. Energy 225, 98–109.
Yang, H.N., Chen, J., Wen, J.J., Tian, H.Z., Liu, X.G., 2016. Composition and sources of PM2.5 around the heating periods of 2013 and 2014 in Beijing: implications for efficient mitigation measures. Atmos. Environ. 124, 378–386.
Yang, J.Y., Shi, B.X., Shi, Y., Marvin, S., Zheng, Y., Xia, G.Y., 2020. Air Pollution Dispersal in High Density Urban Areas: Research on the Triadic Relation of Wind, Air Pollution, and Urban Form, vol. 54. Sustainable Cities and Society.
Yang, S., Wu, H.T., Chen, J., Lin, X.T., Lu, T., 2018. Optimization of PM2.5 estimation using landscape pattern information and land use regression model in zhejiang, China. Atmosphere 9.
Yuan, C., Ng, E., Norford, L.K., 2014. Improving air quality in high-density cities by understanding the relationship between air pollutant dispersion and urban morphologies. Build. Environ. 71, 245–258.
Zhang, D.Q., Wang, Y.P., Zhou, L.P., Yuan, H., Shen, D.G., Alzheimers Dis Neuroimaging, I, 2011. Multimodal classification of Alzheimer's disease and mild cognitive impairment. Neuroimage 55, 856–867.
Zhang, F.Z., Zhou, M., Li, Y.L., Lin, L.Y., Ma, G.W., He, L.H., Chen, S.R., 2021. Characteristics of eco-environmental quality changes in China during the 13th five-year plan period. Environmental Monitoring in China 37, 1–8.
Zhang, J.Y., Zhang, N., Liu, Y.X., Zhang, X.N., Hu, B., Qin, Y., Xu, H.R., Wang, H., Guo, X. X., Qian, J.M., Wang, W., Zhang, P.F., Jin, T., Chu, C.C., Bai, Y., 2018. Root microbiota shift in rice correlates with resident time in the field and developmental stage. Sci. China Life Sci. 61, 613–621.
Zhang, X.F., Wang, Y.L., Li, Z.G., Li, W.F., Ye, M.T., 2007. Preliminary theory of three-dimensional urban landscape ecology. Acta Ecol. Sin. 27, 11.
Zhao, S.P., Yu, Y., Yin, D.Y., He, J.J., Liu, N., Qu, J.J., Xiao, J.H., 2016. Annual and diurnal variations of gaseous and particulate pollutants in 31 provincial capital cities based on in situ air quality monitoring data from China National Environmental Monitoring Center. Environ. Int. 86, 92–106.